VIP Na–CO_2 batteries Very Important Paper

Deutsche Ausgabe: DOI: 10.1002/ange.201602504
Internationale Ausgabe: DOI: 10.1002/anie.201602504

Rechargeable Room-Temperature Na–CO_2 Batteries

*Xiaofei Hu[+], Jianchao Sun[+], Zifan Li, Qing Zhao, Chengcheng Chen, and Jun Chen**

Abstract: *Developing rechargeable Na–CO_2 batteries is significant for energy conversion and utilization of CO_2. However, the reported batteries in pure CO_2 atmosphere are non-rechargeable with limited discharge capacity of 200 mAh g^{-1}. Herein, we realized the rechargeability of a Na–CO_2 battery, with the proposed and demonstrated reversible reaction of $3CO_2 + 4Na \leftrightarrow 2Na_2CO_3 + C$. The battery consists of a Na anode, an ether-based electrolyte, and a designed cathode with electrolyte-treated multi-wall carbon nanotubes, and shows reversible capacity of 60000 mAh g^{-1} at 1 A g^{-1} ($\approx$1000 Wh kg^{-1}) and runs for 200 cycles with controlled capacity of 2000 mAh g^{-1} at charge voltage < 3.7 V. The porous structure, high electro-conductivity, and good wettability of electrolyte to cathode lead to reduced electrochemical polarization of the battery and further result in high performance. Our work provides an alternative approach towards clean recycling and utilization of CO_2.*

Recycling CO_2 in electrochemical energy storage devices, such as metal-CO_2 (M = Li, Na, Mg, Al) batteries, represents a promising "clean" strategy for reducing fossil fuel consumption and restraining the climate effects of CO_2 emissions.[1–5] Furthermore, metal–CO_2 batteries are also potential energy sources for scientific exploration and future immigration on Mars, of which 96% atmosphere is CO_2.[6] Recently, Li–CO_2 batteries have realized rechargeability with 20 cycles under controlled capacity of 1000 mAh g^{-1}, while the decomposition of electrolyte and low round-trip efficiency caused by large polarization at high charge voltage close to 4.5 V remain challenges to be overcome.[7,8] In comparison, the reported Na/Mg/Al–CO_2 batteries were non-rechargeable in pure CO_2, and a limited capacity of $\approx$200 mAh g^{-1} was obtained at room temperature for the Na–CO_2 battery.[9,10] A recent report by Archer's group has shown a rechargeable Na–CO_2/O_2 battery (v/v = 1:1) with voltage window of 2.2–4.7 V.[11] This is the first introduction of CO_2 to a Na–O_2 battery system, but a rechargeable Na–pure CO_2 (denoted Na–CO_2) battery has not been achieved. From theoretical calculations, rechargeable Na–CO_2 batteries show an energy density of 1.1 kWh kg^{-1}, which is comparable to that of rechargeable Na–O_2 batteries.[12,13] In comparison, a Na–CO_2 battery with the reaction of $4Na + 3CO_2 \leftrightarrow 2Na_2CO_3 + C$ ($\Delta rG^{\circ}_m = -905.6$ kJ mol^{-1}) has a lower reaction Gibbs free energy than that proposed for the Li–CO_2 battery reaction ($4Li + 3CO_2 \leftrightarrow 2Li_2CO_3 + C$, $\Delta rG^{\circ}_m = -1081$ kJ mol^{-1}). This means that the lower Gibbs free energy also offers the possibility to realize lower charging potential without electrolyte decomposition. Meanwhile, the non-rechargeability of Na–CO_2 battery is due to challenging issues similar to those found in metal–air batteries, such as gas channel blockage by discharge products, electro-conductivity decrease of cathode materials caused by the deposite of insulating products, and improper cathode surface/interface without sufficient wettability to electrolyte.[14–16] Therefore, the gas cathode of CO_2 needs to be designed to minimize the undesirable clogging, increase the electro-conductivity, and promote the electrochemical reactivity of reversible reactions. In such a gas/liquid/solid system, if a cathode could be designed with the consideration of the above characters, it should be possible to realize the rechargeability of Na–CO_2 batteries with high electrochemical performance.

Herein, we report rechargeable room-temperature Na–CO_2 batteries, consisting of a Na-foil anode, glass fiber separator, ether-based electrolyte, and a tetraethylene glycol dimethyl-treated multi-wall carbon nanotube (t-MWCNT) cathode on Ni mesh without binder addition (Figure 1a). This cathode possesses 3-dimensional tri-continuous porous structure, high electro-conductivity, and good wettability to electrolyte. Through various characterizations, such as in situ Raman spectra and online CO_2-evolution tests, the reversible battery reaction of $3CO_2 + 4Na \leftrightarrow 2Na_2CO_3 + C$ is demonstrated. During discharge, CO_2 reacts with Na to form polycrystalline Na_2CO_3 and amorphous C. In contrast, during charge, the reversible reaction is taking place. The as-prepared Na–CO_2 batteries displayed high electrochemical performance, including large reversible capacity (60000 mAh g^{-1}), high rate capability (4 A g^{-1} with capacity of 4000 mAh g^{-1}), a small discharge/charge voltage gap (0.6 V), and superior cyclability of 200 cycles at 1 A g^{-1}. This study provides fundamental and technological progress towards Na–CO_2 batteries.

In rechargeable Na-CO_2 batteries, the Na anode produces Na^+ during discharge and deposits Na metal during charge, corresponding the anode reaction of $4Na \leftrightarrow 4Na^+ + 4e^-$. The optimized electrolyte is 1M $NaClO_4$ in tetraethylene glycol dimethyl ether (TEGDME) in consideration of its low volatility, intrinsic stability to Na metal, and high ionic conductivity (0.178 S m^{-1}). The key point of this battery system is its cathode, containing a Ni mesh coated by TEGDME-treated MWCNT (t-MWCNT). These electrolyte-treated carbon nanotubes have good wettability to electrolyte, undoubtedly benefiting the cathode reaction

[*] Dr. X. F. Hu,[+] J. C. Sun,[+] Z. F. Li, Q. Zhao, C. C. Chen, Prof. J. Chen
Key Laboratory of Advanced Energy Materials Chemistry
Ministry of Education
and
State Key Laboratory of Elemento-Organic Chemistry
College of Chemistry, Nankai University
Tianjin 300071 (China)
E-mail: chenabc@nankai.edu.cn

[+] These authors contributed equally to this work.

Supporting information for this article can be found under: http://dx.doi.org/10.1002/anie.201602504.

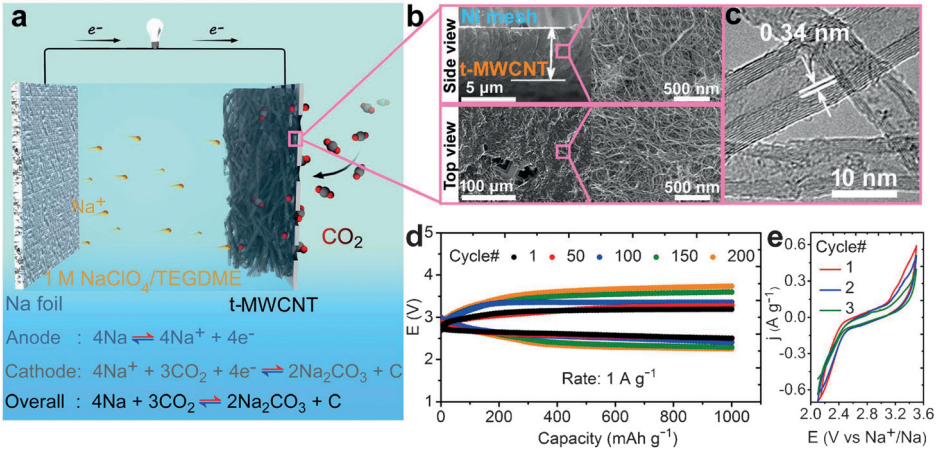

Figure 1. The structure and rechargeability of room-temperature Na–CO_2 batteries. a) Structure of Na–CO_2 batteries with metal Na foil anode, ether-based electrolyte, and t-MWCNT cathode. b) SEM images of cathode from top and and side views. c) HRTEM image of t-MWCNT. d) Discharge and charge profiles of Na–CO_2 batteries at 1 A g^{-1}. e) CV curves of Na–CO_2 batteries with scan rate of 0.1 mV s^{-1}.

($4Na^+ + 3CO_2 + 4e^- \leftrightarrow 2Na_2CO_3 + C$) in the gas/electrolyte/cathode material boundary (surface/interface). This layer with t-MWCNT on the cathode is about 6 μm in thickness and evenly distributed. Moreover, both the side view and top view of this cathode depict a porous cross-linking structure (Figure 1b), which acts as a conductive net and is able to store large amounts of discharge product without blocking air channels. The high resolution transmission electron microscope (HRTEM) image presents the characteristic multi-wall structure of MWCNT with 10–20 walls (Figure 1c). The outer walls of MWCNT are used to nucleate and anchor discharge products, while the retaining inner walls act as a highly conducting network.[17] As designed, once anode and cathode are connected externally, Na–CO_2 batteries with reaction of $4Na + 3CO_2 \leftrightarrow 2Na_2CO_3 + C$ would supply electric energy in discharge and recover in charge (optimization details can be seen in the Supporting Information, Figures S1–S4).

The rechargeable Na–CO_2 battery with a t-MWCNT cathode runs for 200 cycles with controlled capacity of 1000 mAh g^{-1} at a current density of 1 A g^{-1}, demonstrating the high reversibility of this Na–CO_2 system. It exhibits initial and 200th discharge/charge voltage ranges of 2.6–3.2 V and 2.3–3.6 V, respectively (Figure 1d). The discharge voltage is slightly higher than the estimated equilibrium potential of 2.4 V. The relatively low charge voltage plateaus (3.2–3.6 V) are lower than all of the reported Li–CO_2 batteries, and thereby obtaining an initial energy efficiency of 81%. This should be owing to the low Gibbs free energy of Na–CO_2 batteries and well-designed cathode structures. Meanwhile, this low charge voltage also suppresses aprotic electrolyte decomposition, which always occurs above 4 V.[18–20] The cyclic voltammetry (CV) curves depict CO_2-reduction onset potential at 2.4 V and CO_2-revolution onset potential at 3.0 V (Figure 1e), which are consistent with the discharge/charge curves. Moreover, the work window of the Na–CO_2 battery in Ar is 1.5–4.3 V (Figure S5), further suggesting the cycling stability of the Na/$NaClO_4$-TEGDME/t-MWCNT battery system.

The Na–CO_2 battery reaction of $4Na + 3CO_2 \leftrightarrow 2Na_2CO_3 + C$ [labeled as Equation (1)] was demonstrated by various characterizations in Figure 2. An in situ Raman battery was designed to record the reaction progress of discharge and charge. Briefly, a hole in the cathode cap allows Raman signals from the t-MWCNT cathode to be captured, and highly pure CO_2 passes through the inlet and outlet of this battery (Figure 2a). Eleven points among the discharge and charge were selected to collect Raman spectra (inset graph of Figure 2b). The Raman peak at stretching vibrational frequency of 1180 cm^{-1} belonged to Na_2CO_3.[21] This peak initially appeared and increased during discharge. Afterwards, it decreased and disappeared during charge (Figure 2b). The opposite phenomenon corresponds to the reversible formation and decomposition of Na_2CO_3 in Equation (1), which was also detected by XRD patterns (Figure S6). To further confirm this result, X-ray photoelectron spectroscopy (XPS) was applied (Figure 2c). By comparing with the C_{1s} spectra of

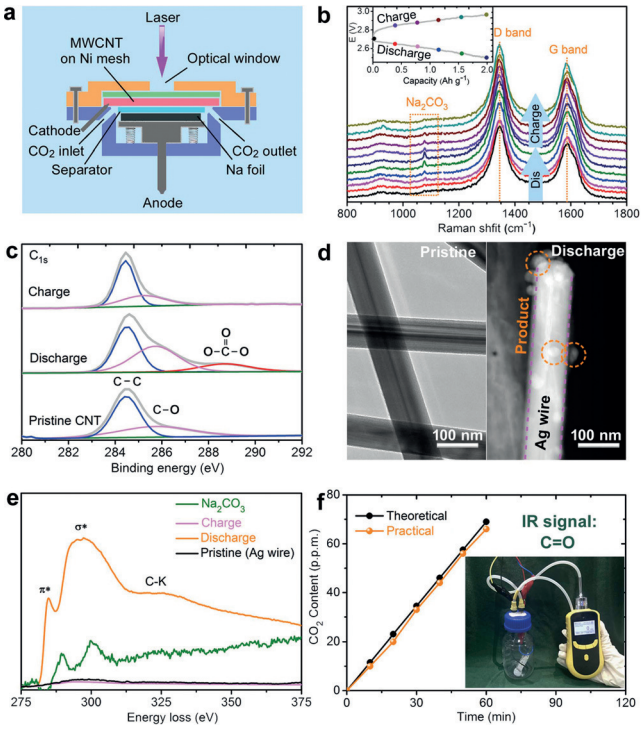

Figure 2. Reaction confirmation of Na–CO_2 batteries, $4Na + 3CO_2 \leftrightarrow 2Na_2CO_3 + C$. a) Design of in situ Raman battery. b) In situ Raman spectrum and corresponding discharge/charge profiles with 11 selective points. Rate: 1 A g^{-1}. c) XPS. d) TEM images of pristine and discharged Ag wire. e) EELS of Ag wire cathode at different states. f) Online CO_2-evolution test.

the pristine t-MWCNT cathode, the discharged cathode depicted a new peak rising at ≈288.70 eV, which can be assigned to the C in carbonate radical of Na_2CO_3.[22] This peak disappeared after charge, indicating the successful removal of Na_2CO_3.

To characterize the existence of carbon in the discharge products, we designed a Ag nanowire cathode applied in a Na–CO_2 battery, given that the carbon nanotube peaks at 1350 (D band) and 1580 cm^{-1} (G band)[23,24] cover the signals of possible carbon products. After discharging at 1 A g^{-1} for 4 h, the cathode was characterized by the electron energy loss spectroscopy (EELS) in a transmission electron microscope (TEM). In sharp contrast with the clean surface of pristine Ag nanowire cathodes (Figure S7), the discharged cathode was deposited by many nanoparticles (Figure 2d). In the EELS result, the visible edges at 280.8 eV correspond to the core-loss K edges of carbon atoms.[25] The peak at 284.8 eV is related to the transition from the 1s orbital to the π* antibonding orbital; the wide peak at 297 eV can be attributed to 1s→σ* transition.[26] According to the visible edge position, the bonding type of carbon atoms is sp^2, which could be from carbon and carbonate. In the standard sample of Na_2CO_3 (green line in Figure 2e), its intensity is relatively weak and visible edge location is 3 eV higher than the discharge product (orange line in Figure 2e). Thus, the EELS signals in the discharge product mainly come from carbon. After the batteries charge, the peak of carbon disappears (pink line in Figure 2e). This indicates the superior reversibility of product carbon. In addition, the results of electrochemical impedance spectroscopy (EIS; Figure S2b) also suggest the existence of carbon, which to some extent lowers the battery resistance.

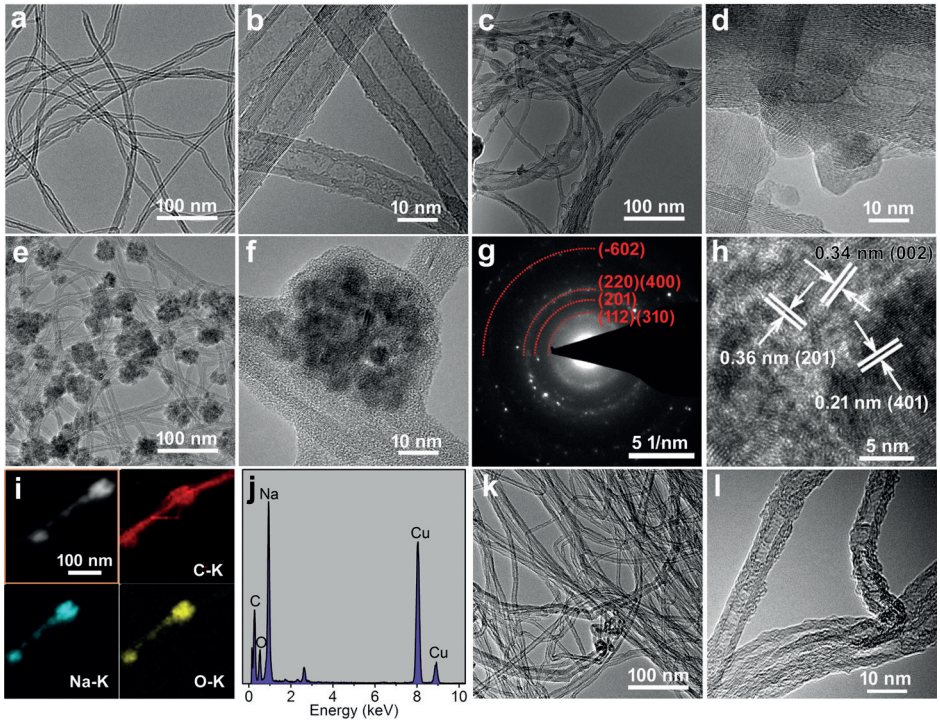

Figure 3. Observation of products from Na–CO_2 batteries. TEM images of MWCNT cathode at different states (1 A g^{-1}). a, b) Pristine state. c, d) Discharge for 1 h. e, f) Discharge for 4 h. g) SAED of (e). h), HRTEM of (f). i, j) EDS and element mapping of 4 h-product. k, l) Charged state of CNT cathode.

To verify whether CO_2 is actually reversibly formed on charging, the evolved gas in a charging process was measured by a portable CO_2-analyzer mounted with a pyroelectric infrared detector (inset photo of Figure 2f), which is highly sensitive to C=O bond stretching vibrations. After discharging at 1 Ag^{-1} for 1 h in pure CO_2 atmosphere, the t-MWCNT cathode was taken out and refabricated to a new battery. Afterwards, the reassembled battery charged at 1 A g^{-1}. The practical CO_2-evolution rate of 11.0 ppm min^{-1} is consistent with the theoretical value (11.5 ppm min^{-1}; Figure 2f). This slight difference probably comes from the dissolution of CO_2 into the electrolyte. The above evidence indicates that the proposed reaction of $4Na + 3CO_2 \leftrightarrow 2Na_2CO_3 + C$ is plausible. Moreover, the cathode with prefilled Na_2CO_3/carbon hybrid shows lower charging voltage by 0.5 V than that with only Na_2CO_3 (Figure S8), further indicating the reactivity of Na_2CO_3/carbon.

The evolution process of discharge products was also characterized (Figure 3). As the Na–CO_2 battery discharged at 1 A g^{-1}, the clean t-MWCNT surface (Figure 3a and 3b) was deposited by nanoparticles (≈15 nm in diameter, 1 h; Figure 3c and 3d). These particles then grew and distributed on the t-MWCNT, but do not interconnect to each other (4 h, Figure 3e). The grape-shaped products are ≈50 nm in diameter and composed of smaller particles (4 h, Figure 3f). The clear fringes observed in selected area electron diffraction (SAED, Figure 3g) indicate the polycrystalline property of the discharge products and present (−602) (201) (401) planes of Na_2CO_3 (JCPDS card no. 86-300). In spite of the presence of some defects, the high resolution transmission electron microscopy (HRTEM) images depict neighboring interlayer distances of 4 h-product, which was consistent with the spacing between the (201) (401) planes of Na_2CO_3 and (002) planes of carbon (JCPDS card no. 41-1487; Figure 3h). These curly (002) planes indicate that the product carbon is not graphene but amorphous graphite carbon. These results confirm the diverse spectrum analysis in Figure 2.

Element mapping of the nano-sized products was collected to obtain the uniformity and local chemical composition of the discharge products (Figure 3i). The C, Na, and O elements were evenly distributed on t-MWCNT and depicted the outline of product particles, which agrees well with the existence of Na_2CO_3 and C. In the energy-dispersive X-ray spectroscopy (EDS) spectra (Figure 3j), elements Na and C

with a relative atomic composition ratio of 2.5:1 rather than 3.8:1 confirmed that the C element not only came from Na_2CO_3 but also from produced carbon. Notably, elements Na and C also emerge on the carbon tube surface between two large product particles, indicating the small crystalline grains that have not expanded. It has been shown that nanosized discharge products provide sufficient interfaces between product and electrolyte, thus facilitating the product decomposition on charging. As expected, the grape shaped product of Na_2CO_3 and C disappear after charging (Figure 3k and 3l). These results further indicate the effective formation and decomposition of Na_2CO_3 and C, namely the rechargeability of the Na–CO_2 battery. Furthermore, we also investigated the influence of discharge current density on product morphology. When discharge current density decreased to 50 mA g^{-1}, the products relating to 4000 mAh g^{-1} capacity were larger particles (50–200 nm) and showed an aggregating trend (Figure S9) in comparison with that at 1 A g^{-1} (Figure 3e). In parallel, the Na anode was also analyzed. SEM images showed that some cracks emerged on the metal Na surface after 50 cycles, and EDS mapping confirmed that the major content was Na (Figure S11).

After confirming the battery reaction and presenting the morphology evolution of products, the superior electrochemical performance of Na–CO_2 batteries was also obtained (Figure 4). When controlling the specific capacity with 2000 and 8000 mAh g^{-1}, the batteries ran 200 and 20 cycles, respectively, with some increase in voltage gap (Figure 4a and 4b). High reversible specific capacities of 60000 mAh g^{-1} at 1 A g^{-1} have also been demonstrated (Figure S10). This equals to ≈1000 Wh kg^{-1} based on the mass (≈0.63 mg) of t-MWCNT and the discharge product. When cycled at 1 A g^{-1}, the initial voltage gap was only ≈0.6 V. At higher rates, the gaps increased to 1.1, 1.4, and 1.7 V, at 2, 3, and 4 A g^{-1}, respectively (Figure 4c). Notably, even at 4 A g^{-1}, the charge voltage was still <3.8 V. A light-emitting diode was shining when connected to a Na–CO_2 battery (inset photo of Figure 4c). Our Na–CO_2 battery was still rechargeable when the loading mass of carbon nanotubes on cathode increased from 71 μg cm^{-2} to 710 μg cm^{-2}, in spite of an elevated overpotential gap (≈1.5 V; Figure 4d). The high rate capability and remarkable cyclability mainly benefit from the 3-dimensional porous structure and high electro-conductivity of t-MWCNT cathode with nanosized discharge products.

In conclusion, rechargeable room-temperature Na–CO_2 batteries were realized in a Na/$NaClO_4$-TEGDME/t-MWCNT system with a unique cathode structure of 3-dimensional porosity, high conductivity, and good wettability to electrolyte. The battery performance outperformed that of all the other reported M–CO_2 batteries (M = Li, Na, Mg, and Al), exhibiting 200 cycles with cut-off 2000 mA g^{-1} at 1 A g^{-1} with initial voltage gap of 0.6 V. A reversible capacity of 60000 mA g^{-1} was obtained, corresponding to an energy density of ≈1000 Wh kg^{-1} based on the mass of t-MWCNT and the discharge products. In addition, the discharge and charge reaction of $4Na + 3CO_2 \leftrightarrow 2Na_2CO_3 + C$ was first demonstrated by various in situ and ex situ characterizations. The results show that rechargeable Na–CO_2 battery chemistry offers a practical opportunity in clean conversion/utilization of CO_2, and in the search for advanced electrochemical energy storage devices.

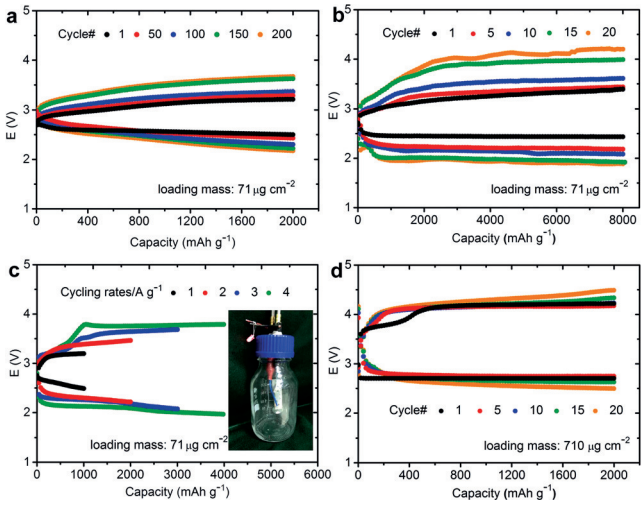

Figure 4. Electrochemical performance of rechargeable room temperature Na–CO_2 batteries. Cyclability at 1 A g^{-1} with controlled capacity of a) 2000 mAh g^{-1} and b) 8000 mAh g^{-1}. c) Rate capability of Na–CO_2 batteries. The inset photo is a LED powered by a coin-type Na–CO_2 battery. d) Cyclability at 1 A g^{-1} with limited capacity of 2000 mAh g^{-1}.

Acknowledgements

This work was supported by NSFC (21231005) and MOE (B12015 and IRT13R30).

Keywords: 3-dimensional porosity · cathode design · CO_2 utilization · multi-wall carbon nanotubes · Na–CO_2 batteries

How to cite: *Angew. Chem. Int. Ed.* **2016**, *55*, 6482–6486
Angew. Chem. **2016**, *128*, 6592–6596

[1] M. Armand, J. M. Tarascon, *Nature* **2008**, *451*, 652–657.
[2] R. D. Richardson, E. J. Holland, B. K. Carpenter, *Nat. Chem.* **2011**, *3*, 301–303.
[3] T. Gasser, C. Guivarch, K. Tachiiri, C. D. Jones, P. Ciais, *Nat. Commun.* **2015**, *6*, 7958–7964.
[4] S. Gao, Y. Lin, X. C. Jiao, Y. F. Sun, Q. Q. Luo, W. H. Zhang, D. Q. Li, J. L. Yang, Y. Xie, *Nature* **2016**, *529*, 68–71.
[5] J. Kothandaraman, A. Goeppert, M. Czaun, G. A. Olah, G. K. S. Prakash, *J. Am. Chem. Soc.* **2016**, *138*, 778–781.
[6] D. R. Williams, *Mars Fact Sheet*. National Space Science Data Center. NASA. Retrieved June 24, **2006**.
[7] Y. Liu, R. Wang, Y. Lyu, H. Li, L. Chen, *Energy Environ. Sci.* **2014**, *7*, 677–681.
[8] Z. Zhang, Q. Zhang, Y. N. Chen, J. Bao, X. L. Zhou, Z. J. Xie, J. P. Wei, Z. Zhou, *Angew. Chem. Int. Ed.* **2015**, *54*, 6550–6553; *Angew. Chem.* **2015**, *127*, 6650–6653.
[9] S. K. Das, S. M. Xu, L. A. Archer, *Electrochem. Commun.* **2013**, *27*, 59–62.
[10] S. M. Xu, S. K. Das, L. A. Archer, *RSC Adv.* **2013**, *3*, 6656–6660.
[11] S. M. Xu, Y. Y. Lu, H. S. Wang, H. D. Abruna, L. A. Archer, *J. Mater. Chem. A* **2014**, *2*, 17723–17729.
[12] C. Xia, R. Black, R. Fernandes, B. Adams, L. F. Nazar, *Nat. Chem.* **2015**, *7*, 496–501.

[13] P. Hartmann, C. L. Bender, M. Vračar, A. K. Dürr, A. Garsuch, J. Janek, P. Adelhelm, *Nat. Mater.* **2013**, *12*, 228 – 232.
[14] F. Y. Cheng, J. Chen, *Nat. Chem.* **2012**, *4*, 962 – 963.
[15] H. D. Lim, K. Y. Park, H. Song, E. Y. Jang, H. Gwon, J. Kim, Y. H. Kim, M. D. Lima, R. O. Robles, X. Lepró, R. H. Baughman, K. Kang, *Adv. Mater.* **2013**, *25*, 1348 – 1352.
[16] Y. X. Hu, T. R. Zhang, F. Y. Cheng, Q. Zhao, X. P. Han, J. Chen, *Angew. Chem. Int. Ed.* **2015**, *54*, 4338 – 4343; *Angew. Chem.* **2015**, *127*, 4412 – 4417.
[17] Y. Y. Liang, H. L. Wang, P. Diao, W. Chang, G. S. Hong, Y. G. Li, M. Gong, L. M. Xie, J. G. Zhou, J. Wang, T. Z. Regier, F. Wei, H. J. Dai, *J. Am. Chem. Soc.* **2012**, *134*, 15849 – 15857.
[18] F. Li, S. C. Wu, D. Li, T. Zhang, P. He, A. Yamada, H. S. Zhou, *Nat. Commun.* **2015**, *6*, 7843 – 7849.
[19] T. Liu, M. Leskes, W. J. Yu, A. J. Moore, L. N. Zhou, P. M. Bayley, G. Kim, C. P. Grey, *Science* **2015**, *350*, 530 – 533.
[20] Q. C. Liu, J. J. Xu, D. Xu, X. B. Zhang, *Nat. Commun.* **2015**, *6*, 7892 – 7899.
[21] M. H. Brooker, *J. Chem. Phys.* **1971**, *54*, 4788 – 4796.
[22] Y. W. Zhu, S. Murali, M. D. Stoller, K. J. Ganesh, W. W. Cai, P. J. Ferreira, A. Pirkle, R. M. Wallace, K. A. Cychosz, M. Thommes, D. Su, E. A. Stach, R. S. Ruoff, *Science* **2011**, *332*, 1537 – 1541.
[23] Y. W. Zhu, S. Murali, W. W. Cai, X. S. Li, J. W. Suk, J. R. Potts, R. S. Ruoff, *Adv. Mater.* **2010**, *22*, 3906 – 3924.
[24] C. Li, X. P. Han, F. Y. Cheng, Y. X. Hu, C. C. Chen, J. Chen, *Nat. Commun.* **2015**, *6*, 7345 – 7353.
[25] O. Stephan, P. M. Ajayan, C. Colliex, Ph. Redlich, J. M. Lambert, P. Bernier, P. Lefin, *Science* **1994**, *266*, 1683 – 1685.
[26] L. J. Ci, L. Song, C. H. Jin, D. Jariwala, D. X. Wu, Y. J. Li, A. Srivastava, Z. F. Wang, K. Storr, L. Balicas, F. Liu, P. M. Ajayan, *Nat. Mater.* **2010**, *9*, 430 – 435.

Received: March 11, 2016
Revised: March 25, 2016
Published online: April 18, 2016

